Advances in Applied Mathematics and Mechanics
Adv. Appl. Math. Mech., Vol. **7**, No. 5, pp. 597-609

DOI: 10.4208/aamm.2013.m454
October 2015

Analysis of Two-Dimensional Thin Structures (From Micro- to Nano-Scales) Using the Singular Boundary Method

Dejian Shen[1,2] and Yan Gu[2,*]

[1] *Department of Civil Engineering, College of Civil and Transportation Engineering, Hohai University, Nanjing 210098, China*
[2] *College of Mathematics, Qingdao University, Qingdao 266071, China*

Received 3 January 2014; Accepted (in revised version) 23 October 2014

Abstract. This study investigates the applicability of the singular boundary method (SBM), a recent developed meshless boundary collocation method, for the analysis of two-dimensional (2D) thin structural problems. The troublesome nearly-singular kernels, which are crucial in the applications of SBM to thin shapes, are dealt with efficiently by using a non-linear transformation technique. Promising SBM results with only a small number of boundary nodes are obtained for thin structures with the thickness-to-length ratio is as small as 1E-9, which is sufficient for modeling most thin layered coating systems as used in smart materials and micro-electro-mechanical systems. The advantages, disadvantages and potential applications of the proposed method, as compared with the finite element (FEM) and boundary element methods (BEM), are also discussed.

AMS subject classifications: 65N15, 65N38

Key words: Singular boundary method, meshless boundary collocation method, method of fundamental solutions, sinh transformation, thin structural problems.

1 Introduction

The method of fundamental solutions (MFS) [1–3] belongs to the family of meshless boundary collocation methods that present remarkable results with a small computational effort. The MFS is easy-to-implement and computationally efficient and thus a competitive alternative for the solution of boundary value problems. However, the traditional MFS requires a fictitious boundary outside the problem domain in order to avoid

*Corresponding author.
Email: guyan1913@163.com (Y. Gu)

singularities of the fundamental solutions. Despite many years of hard research, the determination of the fictitious boundary is largely based on experience and presents the most serious drawback in the MFS applications to real-world problems [4–6].

In recent decades, considerable efforts have been made to mitigate this difficulty associated with the traditional MFS, so that the source points can be placed on the real boundary directly. The developed methods include, but are not limit to, the boundary knot method (BKM) [7], regularized meshless method (RMM) [8], modified method of fundamental solutions (MMFS) [9], boundary collocation method (BCM) [10], and boundary distributed source (BDS) method [11]. The merits and drawbacks of the above-mentioned methods over the traditional MFS for solving elliptic boundary value problems are thoroughly discussed in [12, 13].

In a more recent study, a novel meshless boundary collocation method, called the singular boundary method (SBM), was proposed by Chen and his coworkers [12, 14, 15]. The method cures the perplexing fictitious boundary issue associated with the traditional MFS while inheriting the merits of the latter of being truly meshless, integration-free and easy-to-program. The method also offers several advantages over the classical domain or boundary discretization methods. First of all, it is meshless which means that no mesh, but a mere collection of points is required for the discretization of the problem. Second, it does not involve integration which could be otherwise troublesome, expensive, and complicated, as in the case, for example, the boundary element method (BEM). Thirdly, it is a boundary method which means that it shares all the advantages that the BEM has over domain discretization methods such as the finite element method (FEM). Prior to this study, this method has since been successfully applied to a variety of physical problems, such as two- (2D) and three-dimensional (3D) heat-conduction problems [13, 16, 17], infinite domain problems [18], and elasticity problems [12].

This paper is an extension of our previous work [19] where a non-linear coordinate transformation was proposed and applied to treat boundary layered effect occurring in 2D potential problems. Herein, the developed algorithm is extended to the numerical analysis of 2D thin structural problems. The computer program in Fortran 90 is developed for general thin-structural problems. For the test problems studied, very promising results are obtained when the thickness-to-length ratio of the structure is in the orders of 1E-6 to 1E-9, which is sufficient for modeling most thin layered coating systems in the micro- or nano-scales. A brief outline of the rest of this paper is as follows. The SBM formulation and its implementation are presented in Section 2. Section 3 introduces the transformed SBM formulation for 2D thin structural problems. Followed in Section 4, the accuracy and efficiency of the proposed method are tested on two benchmark 2D thin structural problems, in which the proposed method is compared with the FEM and BEM. Finally, some conclusions and remarks are provided in Section 5.

2 The SBM formulation for 2D potential problems

Without loss of generality, we introduce the SBM formulation of Laplace equation governing potential problems in a 2D domain Ω

$$\nabla^2 u(x)=0, \quad x\in\Omega, \tag{2.1}$$

subject to the following boundary conditions

$$u(x)=\bar{u}(x), \qquad x\in\Gamma_D \ \text{(Dirichlet boundary condition)}, \tag{2.2a}$$

$$q(x)=\frac{\partial u}{\partial n}(x)=\bar{q}(x), \qquad x\in\Gamma_N \ \text{(Neumann boundary condition)}, \tag{2.2b}$$

where u is the potential field, Ω is a bounded domain in R^2 with boundary $\Gamma=\Gamma_D+\Gamma_N$ which we shall assume to be piecewise smooth, n presents the outward normal, and the barred quantities indicate the given values on the boundary.

The basic idea of the SBM is to introduce a concept of the *origin intensity factor* to isolate the singularity of the fundamental solutions, which allows to make coincident the source and collocation points. The SBM formulation for 2D potential problems can be written as follows [19]

$$u(x^i)=\sum_{j=1,j\neq i}^{N}\alpha^j G(x^i,s^j)+\alpha^i u_{ii}, \qquad x^i\in\Gamma_D, \tag{2.3a}$$

$$q(x^i)=\sum_{j=1,j\neq i}^{N}\alpha^j \frac{\partial G(x^i,s^j)}{\partial n_{x^i}}+\alpha^i q_{ii}, \qquad x^i\in\Gamma_N, \tag{2.3b}$$

where $x^i\in\bar{\Omega}=\Omega\cup\Gamma$ and $s^j\in\Gamma$ denote the ith collocation point and the j-th source point, respectively, $\{\alpha^j\}_{j=1}^N$ are the unknown coefficients, and

$$G(x^i,s^j)=-\frac{1}{2\pi}\ln\left\|x^i-s^j\right\|_2 \tag{2.4}$$

is the fundamental solution for 2D Laplace equations. In Eqs. (2.3a) and (2.3b), u_{ii} and q_{ii} are defined as the origin intensity factors, i.e., the diagonal elements of the SBM interpolation matrix. The accurate evaluation of origin intensity factors plays a key role in the present method. After some analytical manipulation [17, 19], the SBM formulation for Neumann boundary conditions (2.3b) can be expressed as

$$q(x^i)=\sum_{j=1,j\neq i}^{N}\alpha^j \frac{\partial G(x^i,s^j)}{\partial n_{x^i}}-\frac{\alpha^i}{l_i}\sum_{j=1,i\neq j}^{N} l_j\frac{\partial G(x^i,s^j)}{\partial n_{s^j}}, \tag{2.5}$$

where l_j denotes the half distance between the source nodes s^{j-1} and s^{j+1} [17], and

$$q_{ii}=-\frac{1}{l_i}\sum_{j=1,j\neq i}^{N} l_j\frac{\partial G(x^i,s^j)}{\partial n_{s^j}}, \tag{2.6}$$

is the aforementioned origin intensity factor for Neumann boundary conditions. The detailed derivation of the above Eqs. (2.5) and (2.6) can be found in [17,19].

The origin intensity factors for Dirichlet boundary conditions can be obtained using the strategy proposed by Sarler [9], where the origin intensity factors are directly set as an average value of the fundamental solution over a line segments. This can be formulated as

$$u_{ii}=\frac{1}{l_i}\int_{\Gamma_s}G(x^i,s)d\Gamma_s=-\frac{1}{2\pi l_i}\int_{\Gamma_s}\ln\left\|x^i-s\right\|_2 d\Gamma_s. \tag{2.7}$$

Then, the average value of the singularity on the boundary can be calculated in closed form [9]

$$u_{ii}=\frac{1}{2\pi}\left(\ln\frac{2}{l_i}+1\right). \tag{2.8}$$

Using the procedures described above, the origin intensity factors on both the Neumann and Dirichlet boundary equations can be extracted out. For the mixed-type boundary problems, a linear combination of Neumann and Dirichlet boundary equations can be made to satisfy the mixed-type boundary conditions. Once all the boundary unknowns are solved, the potential and its derivative at any point inside the domain can be evaluated using the following equations

$$u(y)=\sum_{j=1}^{N}\alpha^j G(y,s^j), \tag{2.9a}$$

$$\nabla u(y)=\sum_{j=1}^{N}\alpha^j \nabla G(y,s^j), \tag{2.9b}$$

where y is a field point located inside the domain, ∇ stands for the partial derivatives with respect to the coordinate component of point y. Employing indicial notation for the coordinates of point y, i.e., y_1, y_2, ∇ can be written as $\partial/\partial y_1$ or $\partial/\partial y_2$.

3 The transformed SBM for thin-structural problems

The numerical difficulty associated with the SBM is the nearly-singular kernels which arise in both crack-like and thin-structural problems. In such cases, the nodes on one side of the boundary usually being too close to the nodes on the opposite side (see Fig. 1), leading to the kernels present various orders of near-singularities. Apart from the boundary nodes, all most all the interior points of a thin structure are very close to the boundary, and therefore, also involve the calculation of nearly singular kernels. Thus, the key point in achieving the required accuracy and efficiency for thin-structure problems using the SBM is the accurate calculation of nearly singular kernels.

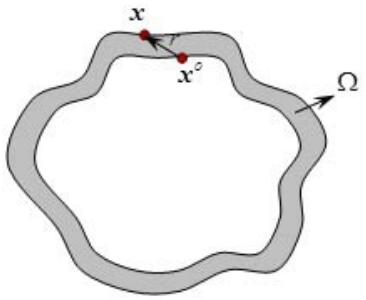

Figure 1: Sketch of a 2D thin structure in which points x^o and x represent boundary points on the adjoining boundaries.

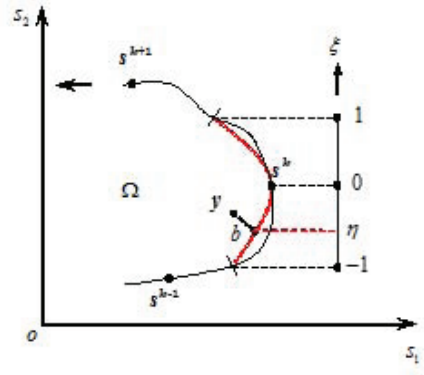

Figure 2: Field point y near the boundary.

In the following, we present an algorithm for the direct calculation of such nearly singular kernels. It should be noted that the method introduced here are very similar to those for solving *boundary layer effect* problems in the SBM, see [19], except for the calculations of boundary unknowns where the proposed regularization method should also be employed. For completeness, we provide all the required formulas. Details on the derivations of some of these formulas can be found in [19].

As shown in Fig. 2, we suppose the field point y is very close to a portion of the boundary containing the point s^k, then we can rewrite Eqs. (2.9a) and (2.9b) as

$$u(y)=\sum_{j=1,j\neq k}^{N}\alpha^j G(y,s^j)+\alpha^k u_k, \tag{3.1a}$$

$$\nabla u(y)=\sum_{j=1,j\neq k}^{N}\alpha^j \nabla G(y,s^j)+\alpha^k q_k, \tag{3.1b}$$

where u_k and q_k are defined as the *nearly singular factors* which should be regularized by using some special treatment. In this study, the nearly singular factors u_k and q_k are directly calculated as an average value of the fundamental solution over a portion of

boundary. This can be formed as

$$u_k=\frac{1}{l_k}\int_{\Gamma_k}G(y,s)d\Gamma_k(s),\quad q_k=\frac{1}{l_k}\int_{\Gamma_k}\nabla G(y,s)d\Gamma_k(s), \tag{3.2}$$

where l_k is the half distance between the source nodes s^{k-1} and s^{k+1}, see Fig. 2. If quadratic boundary element is employed, the distance r between the calculation point and the element can be written as [20]

$$r=\sqrt{(\xi-\eta)^2g(\xi)+b^2}, \tag{3.3}$$

where $\eta\in[-1,1]$ represents the position of the projection of the calculation point onto the element (see Fig. 2), b denotes the shortest distance from the field point to the boundary, $g(\xi)\geq 0$ is a low-order polynomial. The detailed derivation of above equation (3.3) as well as the way how to determine the value of η can be found in [20].

Using the procedure described above, we can rewrite Eq. (3.2) as follows

$$u_k=-\frac{1}{2\pi l_k}\int_{\Gamma_k}\ln r d\Gamma_k(s)=-\frac{1}{4\pi l_k}\int_{-1}^{1}J(\xi)\ln\left[(\xi-\eta)^2g(\xi)+b^2\right]d\xi, \tag{3.4a}$$

$$q_k=-\frac{1}{2\pi l_k}\int_{\Gamma_k}\frac{f(s)}{r^2}d\Gamma_k(s)=-\frac{1}{2\pi l_k}\int_{-1}^{1}\frac{f(\xi)J(\xi)}{(\xi-\eta)^2g(\xi)+b^2}d\xi, \tag{3.4b}$$

where $J(\xi)$ represents the Jacobian of the transformation, $f(\cdot)$ is a low-order polynomial which arises from taking the derivative of the boundary element kernel. For evaluating the integrals shown in Eqs. (3.4a) and (3.4b), Johnston and Elliott [21–23] and Gu and Chen [19,24] suggest a change of integration variable using a sinh function

$$\xi=\eta+b\sinh(k_1t+k_2), \tag{3.5}$$

where k_1 and k_2 are chosen such that the transformation maps $[-1,1]$ onto $[-1,1]$ so that the Gaussian quadrature can be applied in a straightforward fashion to the transformed integral. The Jacobian of transformation (3.5) is given by

$$\frac{d\xi}{dt}=bk_1\cosh(k_1t-k_2). \tag{3.6}$$

Substituting the transformation (3.5) into the integrals (3.4a) and (3.4b) yields

$$u_k=-\frac{bk_1}{4\pi l_k}\int_{-1}^{1}J(t)\cosh(k_1t-k_2)\ln\left\{b^2\left[\sinh^2(k_1t-k_2)g(t)+1\right]\right\}dt, \tag{3.7a}$$

$$q_k=-\frac{k_1}{2\pi l_k b}\int_{-1}^{1}\frac{f(t)J(t)\cosh(k_1t-k_2)}{\sinh^2(k_1t-k_2)g(t)+1}dt. \tag{3.7b}$$

In the above Eqs. (3.7a) and (3.7b), the kernel function $\sinh^2(k_1t-k_2)g(t)+1$ is always greater than 1, since $g(t)$ is a non-negative function as mentioned above. Thus, the integrands are fully regularized and can now be computed straightforward via the standard Gaussian quadrature, even if the value of b is very small.

4 Numerical results and discussions

To verify the method developed above, two benchmark test problems are studied in which SBM solutions are compared with the exact, FEM, or BEM solutions. Here the BEM results are obtained using the procedure developed in [20] for 2D thin structural problems.

4.1 Test problem 1: thin structure with gear wheel shapes

First, we consider the heat diffusion in a thin structure with gear wheel shapes. The outer (Γ_1) and inner (Γ_2) boundaries of the problem, as shown in Fig. 3, can be defined parametrically as

$$\Gamma_1=\left\{(r\cos\theta,r\sin\theta):r=\frac{1}{n^2}\left[n^2+2n+2-2(n+1)\cos(n\theta)\right]+b\right\}, \tag{4.1a}$$

$$\Gamma_2=\left\{(r\cos\theta,r\sin\theta):r=\frac{1}{n^2}\left[n^2+2n+2-2(n+1)\cos(n\theta)\right]\right\}, \tag{4.1b}$$

where $\theta\in[0,2\pi)$, $n=13$ denotes the gear number, b stands for the distance between the outer and inner boundaries.

In this paper, b is defined as the thickness-to-length ratio, i.e., the ratio decreases as b decreases. The analytical solution of this case is available as follows

$$u(x)=e^{x_2}\sin x_1+x_1^2-x_2^2+x_1x_2, \tag{4.2}$$

and the Dirichlet boundary conditions are specified at Γ_1 boundary, while the Neumann boundary conditions are defined at the rest of the boundary.

To solve the problem numerically, $N=200$ evenly distributed source points (in term of the angle parameterization) are chosen on the boundaries, regardless of the thickness of the structure. The calculation point A is placed between the points where the axis x

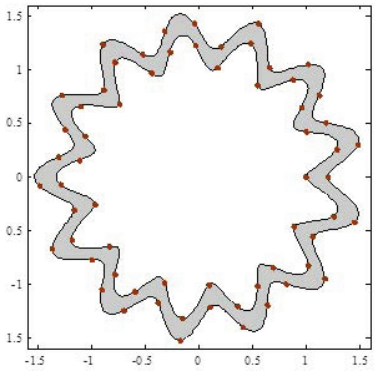

Figure 3: A thin structure with gear wheel shapes.

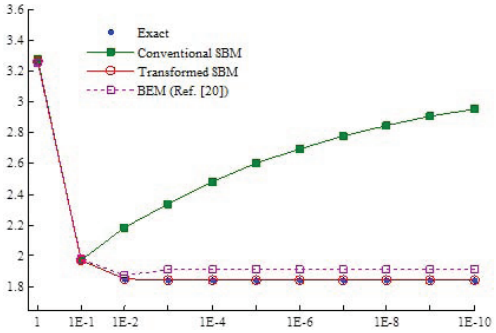

Figure 4: Numerical results for temperatures as functions of different thickness-to-length ratio, thickness-to-length ratio b.

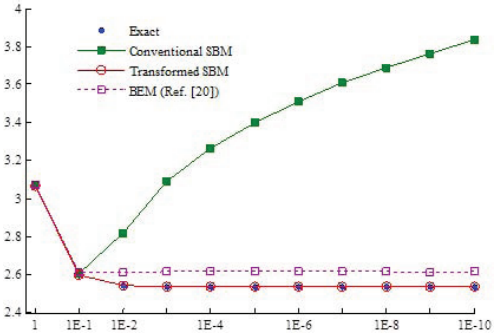

Figure 5: Numerical results for fluxes as functions of different thickness-to-length ratio, thickness-to-length ratio b.

intersects with the curves Γ_1 and Γ_2, i.e., $A=(1+0.5b,0)$. For different thickness-to-length ratios, Figs. 4 and 5 illustrate the numerical results of temperatures $u(x)$ and its partial derivative $\partial u(x)/\partial x_1$ at field point A, respectively. Both the conventional SBM and the proposed transformed SBM are employed for the purpose of comparisons. For the BEM model, the boundary of the thin body is discretized by 80 discontinuous quadratic elements with 240 boundary nodes.

As shown in Figs. 4 and 5, when the thickness-to-length ratio b is not very small $(b\geq 0.1)$, both the SBM schemes are effective and can yield accurate results. However, the conventional SBM performs less satisfactory as the thickness-to-length ratio decreases, i.e., when the value of b is less than 0.1. In stark contrast, results obtained using the proposed algorithm are excellently consistent with the analytical solutions, even in the very unfavorable computational condition $b=1\text{E}-9$ or greater, i.e., when the thickness of the structure is as small as 1E-9 or smaller. In fact, for numerical results shown in Figs. 4 and 5, we found that the largest relative error is less than 2E-3, where the relative error of the numerical solution is defined as

$$Error=\left|\frac{I_{numerical}-I_{exact}}{I_{exact}}\right|, \tag{4.3}$$

where $I_{numerical}$ and I_{exact} denote the numerical and analytical solution at the calculation point, respectively.

It can be also observed that the transformed SBM, in general, outperforms the BEM in terms of overall accuracy. Moreover, it is worth noting that the SBM inherits the merits of meshless method and is computationally far more efficient, easier-to-program and mathematically simple as compared to the BEM.

4.2 Test problem 2: thin structure with amoeba-like shapes

In this case, we consider the heat diffusion in a more complex thin structure with amoeba-like shapes. The outer (Γ_1) and inner (Γ_2) boundaries of the problem, as shown in Fig. 6, can be defined as

$$\Gamma_1=\left\{(r\cos\theta,r\sin\theta):r=e^{\sin\theta}\sin^2(2\theta)+e^{\cos\theta}\cos^2(2\theta)+b\right\}, \tag{4.4a}$$

$$\Gamma_2=\left\{(r\cos\theta,r\sin\theta):r=e^{\sin\theta}\sin^2(2\theta)+e^{\cos\theta}\cos^2(2\theta)\right\}, \tag{4.4b}$$

where $\theta\in[0,2\pi)$, and b is defined as the thickness-to-length ratio which varies in the range of 1E-1$\leq b\leq$1E-10. In this example, Dirichlet and Neumann boundary conditions are specified at Γ_1 and Γ_2 boundaries, respectively, with the following analytical solution

$$u(x)=\sin x_1\cosh x_2\ +x_1^2-x_2^2+x_1x_2. \tag{4.5}$$

The numerical solution has been obtained by the SBM and compared with the FEM. For the SBM model, the total number of $N=100$ boundary nodes are chosen, regardless of the thickness of the structure. The FEM discretization varies according to the structure thickness and, generally, as the thickness decreases, more finite elements are required in order to maintain reasonable element aspect ratio. The calculation point B is placed between the points where the axis x intersects with the curves Γ_1 and Γ_2, i.e., $B=(e+0.5b,0)$.

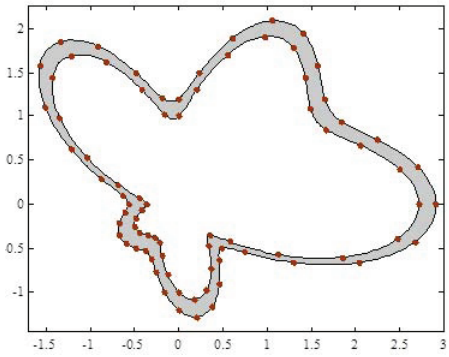

Figure 6: A thin structure with amoeba-like shapes.

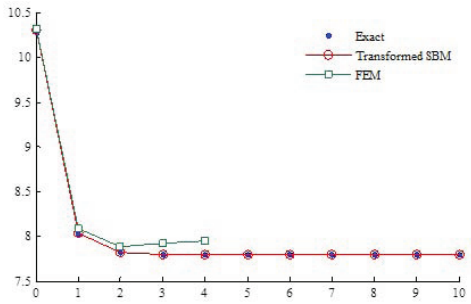

Figure 7: Temperature results for different thickness-to-length ratio (Note that the smallest thickness solved is: $b=10^{-10}$ for SBM and $b=10^{-4}$ for FEM), coating thickness, m, for the ratio $b=10^{-m}$.

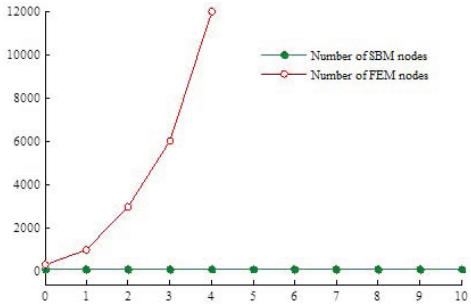

Figure 8: Numbers of nodes required for different thickness-to-length ratio, coating thickness, m, for the ratio $b=10^{-m}$.

Figs. 7 and 8 show the temperature results at point B and the number of nodes needed to achieve solution for both transformed SBM and FEM, respectively. We can see that even for thickness-to-length ratio b in the nano-scale, results of the transformed SBM are still very good, almost reproducing the exact values. Again, the number of SBM nodes does not change across the entire range of thickness-to-length ratio. The solution time and memory requirements are therefore quite modest for the proposed SBM procedure. The FEM solution, however, demonstrates a very different behavior. While the cases with $b \geq 0.1$ are easily solved with the FEM, with a fairly small number of elements, the solution requires significantly more effort when the value of b less than 0.1. Indeed, for $b<$1E-4, the FEM solution becomes infeasible due to memory limitations.

Generally speaking, as has already illustrated in [25–27] or other studies in FEM or BEM literature, the number of FEM elements increases rapidly for thin structures due to aspect ratio limitations, and consequently, the FEM eventually becomes infeasible due to memory constraints. On the other hand, the proposed SBM does not require increasing the number of boundary nodes and can continue to provide accurate results for $b=$1E-10 without any difficulty. Similar results have also been obtained for the flux results, as illustrated in Table 1. Hence we can conclude that, in comparison with existing methods for solving thin structural problems, the transformed SBM could be considered a competitive alternative.

Table 1: Results of partial derivative $\partial u/\partial x_1$ at point B using SBM, BEM, and FEM.

b	Exact	Conventional SBM	Transformed SBM	BEM Ref. [20]	FEM
1.0E-1	4.6054	5.8743	4.6145	4.6214	4.6185
1.0E-2	4.5327	×	4.5369	4.5769	4.5962
1.0E-3	4.5256	×	4.5259	4.5821	4.5608
1.0E-4	4.5249	×	4.5247	4.5953	4.6173
1.0E-5	4.5248	×	4.5246	4.5997	×
1.0E-6	4.5248	×	4.5246	4.6001	×
1.0E-7	4.5248	×	4.5245	4.6012	×
1.0E-8	4.5248	×	4.5246	4.6098	×
1.0E-9	4.5248	×	4.5249	4.6114	×
1.0E-10	4.5248	×	4.5246	4.6953	×

5 Conclusions and remarks

This paper investigates the applicability of the SBM for the analysis of 2D thin structures in micro- and nano-scales. It is shown that the SBM, with proper treatment of nearly-singular kernels, will be very accurate and efficient in modeling 2D thin structural problems. Compared with BEM and FEM, the developed SBM has the following attractive features:

(1) Using only boundary discretization instead of domain discretization, the SBM does not suffer from thickness or aspect ratio issues associated with FEM-based methods. Therefore, the number of SBM nodes can be held constant as described in example, without any loss in solution accuracy as the thickness decreases.

(2) All SBM interpolation matrix elements are directly calculated in the strong-form fashion and only near-singular terms are determined by numerical integration. Therefore, the develop method remains a strong form approach and is computationally far more efficient, easier-to-program and mathematically simple as compared to the BEM.

All these features of the SBM approach make it very attractive to the modeling and analysis of thin structural problems. Applications of the proposed SBM approach to thin structural problems can be found in many areas such as thin-layered coating systems, turbine blades, rudders and various containers, where other computational modes, such as the FEM, become inefficient or fail. Some work along this line is already underway and will be reported in a subsequent paper.

Acknowledgements

The work described in this paper was supported by the National Natural Science Funds of China (No. 11402075), the National Basic Research Program of China (973 Project

No. 2010CB832702), the National Science Funds for Distinguished Young Scholars of China (No. 11125208), the open foundation of State Key Laboratory for Disaster Reduction in Civil Engineering of Tongji University (No. SLDRCE 13-MB-05), and the Fundamental Research Funds for Central Universities (No. 2014B07114).

References

[1] G. Fairweather and A. Karageorghis, *The method of fundamental solutions for elliptic boundary value problems,* Adv. Comput. Math., 9 (1998), pp. 69–95.
[2] A. Karageorghis, D. Lesnic and L. Marin, *A survey of applications of the MFS to inverse problems,* Inverse. Probl. Sci. Eng., 19 (2011), pp. 309–336.
[3] C. S. Chen, H. A. Cho and M. A. Golberg, *Some comments on the ill-conditioning of the method of fundamental solutions,* Eng. Anal. Bound. Elem., 30 (2006), pp. 405–410.
[4] L. Marin, *A meshless method for solving the cauchy problem in three-dimensional elastostatics,* Comput. Math. Appl., 50 (2005), pp. 73–92.
[5] C. S. Chen, *The method of fundamental solutions for non-linear thermal explosions*, Commun. Numer. Methods. Eng., 11 (1995), pp. 675–681.
[6] C.-S. Liu, *An equilibrated method of fundamental solutions to choose the best source points for the Laplace equation*, Eng. Anal. Bound. Elem., 36 (2012), pp. 1235–1245.
[7] W. Chen and M. Tanaka, *A meshless, integration-free, and boundary-only RBF technique,* Comput. Math. Appl., 43 (2002), pp. 379–391.
[8] D. L. Young, K. H. Chen and C. W. Lee, *Novel meshless method for solving the potential problems with arbitrary domain,* J. Comput. Phys., 209 (2005), pp. 290–321.
[9] B. Sarler, *Solution of potential flow problems by the modified method of fundamental solutions: Formulations with the single layer and the double layer fundamental solutions*, Eng. Anal. Bound. Elem., 33 (2009), pp. 1374–1382.
[10] J. T. Chen, M. H. Chang, K. H. Chen and S. R. Lin, *The boundary collocation method with meshless concept for acoustic eigenanalysis of two-dimensional cavities using radial basis function,* J. Sound. Vib., 257 (2002), pp. 667–711.
[11] Y. J. Liu, *A new boundary meshfree method with distributed sources,* Eng. Anal. Bound. Elem., 34 (2010), pp. 914–919.
[12] Y. Gu, W. Chen and C.-Z. Zhang, *Singular boundary method for solving plane strain elastostatic problems,* Int. J. Solids. Struct., 48 (2011), pp. 2549–2556.
[13] W. Chen and Y. Gu, *An improved formulation of singular boundary method,* Adv. Appl. Math. Mech., 4 (2012), pp. 543–558.
[14] Y. Gu, W. Chen and X. Q. He, *Improved singular boundary method for elasticity problems,* Comput. Struct., 135 (2014), pp. 73–82.
[15] Y. Gu, W. Chen, Z. J. Fu and B. Zhang, *The singular boundary method: Mathematical background and application in orthotropic elastic problems,* Eng. Anal. Bound. Elem., 44 (2014), pp. 152–160.
[16] W. Chen and F. Z. Wang, *A method of fundamental solutions without fictitious boundary,* Eng. Anal. Bound. Elem., 34 (2010), pp. 530–532.
[17] Y. Gu, W. Chen and X. Q. He, *Singular boundary method for steady-state heat conduction in three dimensional general anisotropic media,* Int. J. Heat. Mass. Transf., 55 (2012), pp. 4837–4848.
[18] Y. Gu and W. Chen, *Infinite domain potential problems by a new formulation of singular boundary method,* Appl. Math. Model., 37 (2013), pp. 1638–1651.

[19] Y. GU, W. CHEN AND J. ZHANG, *Investigation on near-boundary solutions by singular boundary method,* Eng. Anal. Bound. Elem., 36 (2012), pp. 1173–1182.
[20] Y. M. ZHANG, Y. GU AND J. T. CHEN, *Boundary element analysis of 2D thin walled structures with high-order geometry elements using transformation,* Eng. Anal. Bound. Elem., 35 (2011), pp. 581–586.
[21] B. M. JOHNSTON, P. R. JOHNSTON AND D. ELLIOTT, *A sinh transformation for evaluating two-dimensional nearly singular boundary element integrals,* Int. J. Numer. Methods. Eng., 69 (2007), pp. 1460–1479.
[22] P. R. JOHNSTON AND D. ELLIOTT, *A sinh transformation for evaluating nearly singular boundary element integrals*, Int. J. Numer. Methods. Eng., 62 (2005), pp. 564–578.
[23] B. M. JOHNSTON AND P. R. JOHNSTON, *A comparison of transformation methods for evaluating two-dimensional weakly singular integrals,* Int. J. Numer. Methods. Eng., 56 (2003), pp. 589–607.
[24] Y. GU, W. CHEN AND C. ZHANG, *Stress analysis for thin multilayered coating systems using a sinh transformed boundary element method,* Int. J. Solids. Struct., 50 (2013), pp. 3460–3471.
[25] J. F. LUO, Y. J. LIU AND E. J. BERGER, *Analysis of two-dimensional thin structures (from micro- to nano-scales) using the boundary element method,* Comput. Mech., 22 (1998), pp. 404–412.
[26] G. R. LIU, J. D. ACHENBACH, J. O. KIM AND Z. L. LI, *A combined finite element method/boundary element method technique for $V(z)$ curves of anisotropic-layer/substrate configurations,* J. Acoust. Soc. Am., 92 (1992), pp. 2734–2740.
[27] V. SLADEK, J. SLADEK AND M. TANAKA, *Nonsingular BEM formulations for thin-walled structures and elastostatic crack problems,* Acta. Mech., 99 (1993), pp. 173–190.